New Journal of Physics
An Institute of Physics and Deutsche Physikalische Gesellschaft Journal

# Stabilization of Si-based cage clusters and nanotubes by encapsulation of transition metal atoms

**Antonis N Andriotis**[1], **Giannis Mpourmpakis**[2], **George E Froudakis**[2] **and Madhu Menon**[3,4]

[1] Institute of Electronic Structure and Laser, Foundation for Research and Technology-Hellas, PO Box 1527, 71110 Heraklio, Crete, Greece
[2] Department of Chemistry, University of Crete, PO Box 1470, Heraklio Crete, 71409, Greece
[3] Department of Physics and Astronomy, University of Kentucky, Lexington, KY 40506-0055, USA
[4] Center for Computational Sciences, University of Kentucky, Lexington, KY 40506-0045, USA
E-mail: andriot@iesl.forth.gr, frudakis@chemistry.uoc.gr and madhu@ccs.uky.edu

*New Journal of Physics* **4** (2002) 78.1–78.14 (http://www.njp.org/)
Received 20 June 2002, in final form 11 September 2002
Published 23 October 2002

**Abstract.** The encapsulation of metal atoms within Si-based cage clusters leads to stable metal-encapsulated Si cage clusters (Si-cc). The present work investigates the effect of encapsulation of transition metal atoms (TMAs). We show that the filling factor of the d-band of the TMA is the dominant factor determining the structural configuration of the Si-cc. This results in a contrasting bonding and magnetic behaviour of the endohedral Ni and V atoms. The size of the encapsulated atom is found to play a minor role. Both Ni and V were found to stabilize Si-cc. More significantly, we show that both Ni and V, in the form of one-dimensional chains, can stabilize Si nanotubes encapsulating the Ni or the V chain. Our results also show that these metal-encapsulated Si nanotubes have small conduction gaps and become metallic at infinite length.

## 1. Introduction

The successful synthesis of metallofullerenes (MFs) (for a recent review see [1]), and the recognition of the tremendous potential of the doping atoms to fine-tune the electronic properties


1367-2630/02/000078+14$30.00

of MFs, have prompted intense research activity in the synthesis and study of metal-doped Si clusters. Such studies are motivated by the numerous applications that metal-doped Si structures have found in microelectronics.

It is now well known that Si cage clusters (Si-cc) of the fullerene type are not stable [2]. However, recent studies [3]–[8] have reported findings confirming the stability of $M_nSi_m$, binary clusters with M being either a transition metal (TM) or Cu. These studies have also provided evidence that it is possible to stabilize Si-cc by encapsulation of metal atoms. In particular, Hiura *et al* [3] were able to synthesize stable metal-encapsulating Si-cc ions. In their experiment the metal ion was found to serve as a reaction site, nucleating a cluster of Si atoms until it was completely covered. Although the starting metal atoms were ionized positively, they became neutral after encapsulation by Si. Furthermore, the number of Si atoms that formed the cage cluster depended on the chemical identity of the metal atom. The transition metal atoms (TMAs) observed to undergo complete covering by Si atoms included Cr, Mo, W, Hf, Ta, Re, Ir, Nb, Mo, Co and Ni.

Hiura *et al* also provided theoretical support for their findings by performing *ab initio* optimizations for a $WSi_{12}$ cluster. They found a W-encapsulating regular hexagonal (h) $Si_{12}$ prism to be the most stable geometry for this binary system. Additionally, they also found a basket-like structure ($C_{2v}$ symmetry) to be a local minimum, although 1 eV higher in energy. Following this work Kumar and Kawazoe [6, 7], using first-principles-based calculations incorporating the cage-shrinkage method, have predicted the existence of stable $MSi_n$ clusters with $M = Zr$, Hf, Ti, Ru, Os, Cr, Mo and W and $n = 14$–17. The shape of the cage of the low lying cage structures were found to be of fullerene-like (f), Frank–Kasper (FK) polyhedral, cubic (c) and decahedral (d) types [6, 7]. In table 1 we have tabulated the reported metal-encapsulated Si-cc.

Detailed study of metal-encapsulated Si-cc using molecular dynamics simulations by the present authors has revealed that the stability of Si-cc induced by metal encapsulation can be extended to Si-based nanotubes [9]. Furthermore, we have shown that a Si nanotube stabilized by a chain of Ni atoms exhibits an energy gap at the Fermi energy, $E_F$, which becomes vanishingly small as the length of the tube increases. In extending that work it has been found (as will be shown later) that similar trends are found in the case of Si-cc encapsulating other TMAs as well. Thus, it has become apparent that Si-based nanotubes can be built up from small Si-cc units, the latter stabilized by the encapsulation of TMAs. The symmetry (and type) of these units, however, appears to be dictated by the occupancy of the d shell of the TMAs.

From the present study three additional important features can be deduced. The first is that the TMA is over-coordinated—a feature that is associated with stabilization of the Si cages; the stabilization seems to be dependent on the type rather than the size of the encapsulated atom. The second is based on the observation that by varying the type of the endohedral atom, one can control the highest occupied molecular orbital–lowest unoccupied molecular orbital (HOMO–LUMO) gap, enabling bandgap engineering. Finally, the third feature is the observation that most of the encapsulated magnetic metal atoms lose their magnetic moment upon encapsulation by the Si cage.

In the present work we present a theoretical study of the encapsulation of Ni and V by Si-cc and compare our results with those recently reported by others. After a brief review of the computational methods used, we proceed with the presentation of the results. Finally, we end with a discussion of our results followed by conclusions.

**Table 1.** Reported optimum structures for Si-cc of the form $MSi_m$ with M = Ti, Zr, Hf, V, Cr, Mo, W, Fe, Ru, Os, Ni and $m$ = 12, 14, 15, 16, 17 and 20. c stands for cubic, d for decahedral, f for fullerene-like and FK for the polyhedral FK structure respectively.

| Element | $MSi_{12}$ | $MSi_{14}$ | $MSi_{15}$ | $MSi_{16}$ | $MSi_{17}$ | $MSi_{20}$ |
|---|---|---|---|---|---|---|
| Ti | | | c[a] | FK[b] | | |
| Zr | | | c(f)[a] | f[b] | | $I_h$[d] |
| Hf | | | c(f)[a] | f (FK)[b] | | |
| V | $D_{6h}$[e] | | | | | |
| Cr | | d[a] | c(f)[a] | f[a] | f, FK, d[a] | |
| Mo | | d[a] | c(f)[a] | f[a] | d, f, FK[a] | |
| W | $C_{6v}$, $(C_{2v})$[c] | d[a] | c(f)[a] | f[a] | f, d, FK[a] | |
| Fe | | c[b] | | | | |
| Ru | | c(f)[b] | c[a] | | | |
| Os | | c, f[b] | c[a] | | | |
| Ni | $C_{5v}$[e,f] | | | | $C_{5v}$[e,f] | |

[a] Reference [7].
[b] Reference [6].
[c] Reference [3].
[d] Reference [25].
[e] Present work and [9].
[f] The $C_{5v}$ symmetry was also found in the Ni-stabilized $Ni_2Si_{17}$, $Ni_3Si_{22}$, $Ni_7Si_{42}$ and $Ni_{15}Si_{82}$ clusters; see [9] and figure 1.

## 2. Computational approach

In this section we give brief overviews of our theoretical simulation method.

### *2.1. Tight-binding molecular dynamics methodology*

The details of our tight-binding molecular dynamics (TBMD) scheme can be found in [10]. Here we give a brief overview.

The total energy $U$ is written in its general form as a sum of several terms [10],

$$U = U_{el} + U_{rep} + U_0, \tag{1}$$

where $U_{el}$ is the sum of one-electron energies $E_n$ for the occupied states:

$$U_{el} = \sum_{n}^{occ} E_n. \tag{2}$$

In the tight-binding scheme $E_n$ is obtained by solving the characteristic equation:

$$(\boldsymbol{H} - E_n\mathbf{1})\boldsymbol{C}^n = 0, \tag{3}$$

where $\boldsymbol{H}$ is the Hamiltonian of the system.

The Hellmann–Feynman theorem for obtaining the electronic part of the force is given by [10],

$$\frac{\partial E_n}{\partial x} = \boldsymbol{C}^{n\dagger}\frac{\partial \boldsymbol{H}}{\partial x}\boldsymbol{C}^n. \tag{4}$$

The total energy expression also derives contributions from ion–ion repulsion interactions. This is approximated by a sum of pairwise repulsive terms and included in $U_{rep}$. This sum also contains the corrections arising from the double counting of electron–electron interactions in $U_{el}$ [10]. $U_0$ is a constant that merely shifts the zero of energy. The contribution to the total force from $U_{rep}$ is rather straightforward. One can then easily perform molecular dynamics simulations by numerically solving Newton's equation,

$$m\frac{\mathrm{d}^2x}{\mathrm{d}t^2} = F_x = -\frac{\partial U}{\partial x} \tag{5}$$

to obtain $x$ as a function of time.

Our TBMD scheme for a binary system consisting of elements A and B is based on a minimal set of five adjustable parameters for each pair (A, A), (B, B) and (A, B). These parameters are determined by fitting to experimental data for quantities such as the bond length, the vibrational frequency and the binding energy of the dimers $\mathrm{A}_2$, $\mathrm{B}_2$ and AB, the cohesive energy of the corresponding bulk states of the A, B and AB materials and the energy level spacing of the lowest magnetic states of the dimer and trimer binary clusters consisting of atoms of A and B type. In the absence of experimental data, we fit to the data of small clusters obtained using *ab initio* methods as described in the following subsection. We find that only five parameters are required in the case of a system consisting of a single species. The same approach also works for generalization to a system containing more than two kinds of atom.

The fixed set of TB parameters [11] are obtained from the universal scheme proposed by Harrison [12], with parameters suitably scaled with respect to the interatomic distances [10].

### *2.2. Ab initio approach*

Our TBMD simulations for the large clusters were based on results obtained from small clusters, the latter obtained by *ab initio* calculations. The *ab initio* calculations were performed using the GAUSSIAN 98 program package [13] and includes density functional theory (DFT) calculations with the three-parameter hybrid functional of Becke using the Lee–Yang–Parr correlation functional (B3LYP). Several atomic basis sets were used for the dimers Ni–Si and V–Si. In particular, we used basis sets of double- and triple-zeta quality augmented by polarization functions (6-31G$^\star$ and 6-311G$^\star$ respectively) as well as sets that include relativistic corrections (LanL2DZ) for Ni and V. For the larger clusters (up to size of $\mathrm{M_3Si_{26}}$, M = Ni, V), we employed the B3LYP/LanL2DZ level of approximation. Up to this level, our *ab initio* obtained structures are fully optimized without any symmetry constraints.

## 3. Encapsulation of Ni and V atoms/clusters

Our studies on the interaction of TMAs with low-dimension carbon materials have shown contrasting bonding behaviours of 3d TMAs with graphite, single-wall carbon nanotubes (SWCNs) and $\mathrm{C_{60}}$ [14]–[18]. In particular, it was found that V on both graphite and $\mathrm{C_{60}}$ exhibits a preference to act as an $\eta^6$ ligand, in contradistinction with Ni which acts

as an $\eta^2$ or $\eta^3$ ligand [15, 16], in agreement with the experimental findings for both Ni and V interacting with $C_{60}$ [19]–[23]. (The symbol, $\eta^k$, $k$ an integer, denotes bonding in which the metal atom (Ni, V) forms $k$-bonds with carbon atoms.) From these results it is clear that the bonding characteristics between a TMA and a low-dimension carbon surface depend on the occupancy of the d shell of the TMA. It is worthwhile to investigate if these same contrasting bonding behaviours are also present in the case of interaction of TMAs with Si.

The accuracy of our TBMD results (as compared with that of the *ab initio* method) has been verified in the case of the icosahedral $Si_{12}$ cluster stabilized by a Ni atom located at the centre of the icosahedron. The optimized geometries obtained without any symmetry constraints by both methods had the same $C_{5v}$ symmetry, but differed slightly in bond lengths. The *ab initio* optimized $NiSi_{12}$ cluster had an average Ni–Si bond length of 2.63 Å and Si–Si bond length of 2.55 Å. The corresponding bond lengths for the TBMD relaxed $NiSi_{12}$ cluster were 2.50 and 2.56 Å, respectively. The cluster has spherical geometry and the central Ni has 12 Si neighbours, while each Si has six neighbours.

In the following we present the results of two sets of calculations. The first deals with the encapsulation of Ni atoms within Si-cc and the other to the encapsulation of V. In both cases we start with *ab initio* calculations on small $M_nSi_m$ clusters with $n + m \leq 4$ and $M = Ni$, V. These sets of calculations are used to fit the set of adjustable parameters used in our TBMD computer code. Subsequently, we perform both *ab initio* and TBMD simulations for medium-size clusters followed by TBMD simulations for large clusters (with number of atoms greater than 20).

### *3.1. Encapsulation of Ni*

The results of our *ab initio* calculations for the NiSi dimer were reported in [24]. For completeness, we include them in table 2. According to that work, the ground state of the NiSi dimer is a singlet state well separated from states of higher multiplicity. As will be shown later, this is not the case for the VSi dimer for which an extensive search for the basis set is necessary to obtain converged results. Recently, in another report [9], we presented preliminary results for the effect of Ni encapsulation on the stability of Si-cc. There it was shown that for the smallest cage clusters possible, the structures with $C_{5v}$ symmetry were energetically most stable for the Ni-encapsulated Si cages. Expanding on these findings, we found that larger $Ni_mSi_n$ clusters (i.e., with $n + m \geq 19$) can be made stable by taking a cylindrical form with $C_{5v}$ symmetry by the encapsulation of Ni atoms arranged in a one-dimensional chain along the symmetry axis. These high-symmetry $Ni_mSi_n$ structures exhibit the following properties.

- In their ground state, the tubes are of $C_{5v}$ symmetry and $Ni_mSi_{5m+7}$ form, $m \geq 1$.
- Each Ni atoms has 12 neighbours, i.e., 11 Si and one Ni, or ten Si and two Ni atoms.
- The Si–Si bond length is larger than the covalent Si–Si bond in bulk Si. In particular, the Si–Si bond lengths were found to be around 2.55 Å while the Ni–Si bonds lengths were near 2.6 Å.
- The tubes exhibit a small gap at $E_F$; this gets smaller as the length of tube increases. At infinite length, the tubes become metallic.
- The encapsulated Ni atoms do not exhibit appreciable magnetic moment; it is mostly passivated.
- No appreciable charge transfer is found.

**Table 2.** *Ab initio* results for the dimers Ni–Si and V–Si obtained at various levels of approximation. The results include the energy difference of the spin states, the bond length, the vibration frequency and the charge state of the dimers.

| Cluster (basis set) | $2S+1$ | Energy[a] (eV) | Bond length (Å) | Frequency ($cm^{-1}$) | Charge state[b] for metal ($\|e\|$) |
|---|---|---|---|---|---|
| Ni–Si (B3LYP) | 1 | 0.00 (−1797.666515) | 2.142[c] | 400[c] | 0.25[c] |
| Ni–Si (CCSDT) | 1 | 0.00 (−1795.913801) | 2.124[d] | | |
| V–Si (6-31G$^\star$) | 2 | 0.18 (−1233.258605) | 2.41 | 305.4 | 0.31 |
| | 4 | 0.00 (−1233.265445) | 2.34 | 342.1 | 0.26 |
| | 6 | 0.12 (−1233.260761) | 2.42 | 349.7 | 0.27 |
| V–Si (6-311G$^\star$) | 2 | 0.07 (−1233.326805) | 2.38 | 291.3 | 0.47 |
| | 4 | 0.00 (−1233.329263) | 2.22 | 349.1 | 0.46 |
| | 6 | 0.41 (−1233.314362) | 2.28 | 359.8 | 0.43 |
| V–Si (6-311G$^\star$) and LanL2DZ | 2 | 0.07 (−360.684548) | 2.32 | 295.6 | 0.24 |
| | 4 | 0.00 (−360.687009) | 2.26 | 333.2 | 0.20 |
| | 6 | 0.25 (−360.677999) | 2.31 | 335.1 | 0.15 |

[a] We have assigned the zero-energy level to the energetically most optimum configuration within the indicated level of approximation; absolute energies (in Hartrees) are given in parentheses below the relative energy (the latter given in eV).
[b] Positive charge state means that the metal loses electrons to the surrounding Si atoms.
[c] Results obtained within the B3LYP/6-311G$^\star$ method; see [24].
[d] Results obtained within the CCSD(T)/6-311G$^\star$ method; see [24].

In figure 1(a) we show a finite $Ni_{15}Si_{82}$ tube fully relaxed using the TBMD method. Figure 2 shows the current–voltage ($I$–$V$) characteristic of the $Ni_{15}Si_{80}$ nanotube in contact with two semi-infinite metal leads made of Ni(001). The $Ni_{15}Si_{80}$ tube is the same nanotube as shown in figure 1(a) but without the capping Si atoms at both ends. In the inset of figure 2 we show the transmission function $T(E)$. These calculations are based on a combination of the TBMD method and our newly proposed surface Green function matching (SGFM) method as outlined in [26]. Briefly, this method relies on Landauer's [27] expression for $T(E)$ and Datta's [28] computational scheme for transport, the latter suitably modified to incorporate the Inglesfield method for embedding [26, 29]–[32]. In particular, we consider the case of a finite length SWCN

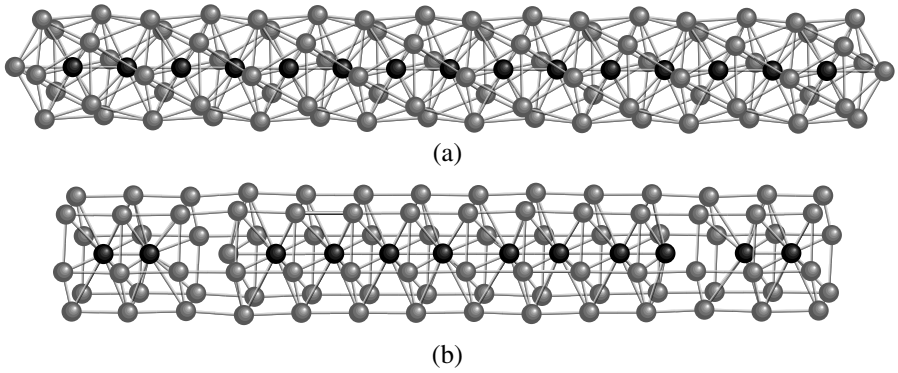


**Figure 1.** Si-based tubes of finite length: (a) $Ni_{15}Si_{82}$ tube of $C_{5v}$ symmetry; (b) $V_{13}Si_{84}$ tube of $D_{6h}$ symmetry. The Ni and/or V atoms are shown dark.

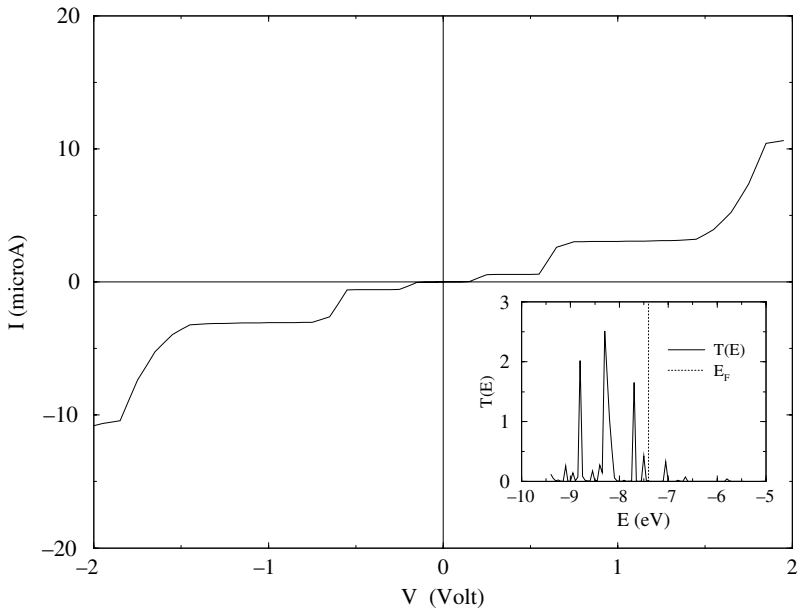


**Figure 2.** The $I$–$V$ characteristic of the Si nanotube shown in figure 1(a) (without the capping atoms at the tube ends) calculated according to equations (6)–(9) under a symmetric bias. The tube is in contact with two semi-infinite metal leads made of Ni(001). In the inset, the calculated transmission function $T(E)$ is shown.

connected at both ends to semi-infinite metallic leads. We denote by $L$ $(R)$ the left (right) lead, respectively. Within our embedding scheme, the effect of metallic leads is replaced by suitably calculated self-energies, $\Sigma_L(E)$ and $\Sigma_R(E)$ for the left and right metallic leads, respectively. These self-energies depend on the energy $E$. Having constructed the self-energies, one can obtain the Green function $G_C(E)$ of the tube in contact with the metallic leads as follows:

$$G_C = (E - H_C - \Sigma_L - \Sigma_R)^{-1}, \tag{6}$$

where $H_C$ is the Hamiltonian of the isolated tube.

Having evaluated $G_C$ the transmission function, $T(E)$, can now be obtained from the following equation [28]:

$$T(E, V_b) = \mathrm{tr}[\Gamma_L G_C \Gamma_R G_C^\dagger], \tag{7}$$

where

$$\Gamma_j(E; V_b) = \mathrm{i}(\Sigma_j - \Sigma_j^\dagger), \qquad j = L, R. \tag{8}$$

Having obtained $T(E, V_b)$, we proceed with the evaluation of the $I$–$V$ characteristic of the tube utilizing the following formula for calculating the current [28]:

$$I(V_b) = \frac{2e}{h} \int_{-\infty}^{+\infty} T(E, V_b)[f_E(\mu_L) - f_E(\mu_R)]\,\mathrm{d}E, \tag{9}$$

where $\mu_i = E_F - eV_i$; $i = L, R$, $V_L$ and $V_R$ are applied voltages on the left and the right metal leads, respectively, $e > 0$ is the electron charge, $E_F$ the Fermi energy of the free tube and $f_E(\mu)$ the Fermi distribution. In the following we set $V_b = V_L - V_R$ to be the bias voltage.

In figure 2 it is worth noting the existence of a small conduction gap at $E_F$ of the order of 0.3 eV. Very recently, calculations on Si nanowires (built up from both tricapped and uncapped trigonal prism units) have revealed gaps of the same order and which also tend to vanish as the tube length increases [8].

### *3.2. Encapsulation of V*

We begin the study of V encapsulation in Si-cc by investigating the VSi dimer. These calculations are required in order to generate the necessary data (because of the absence of experimental ones) for fitting our TBMD parameters. The study of this dimer poses a considerable challenge when compared to the corresponding case of NiSi with regards to the converged results for the basis set. For this reason we experimented with various sets of basis functions and our results are tabulated in table 2. From these it is apparent that the ground state of VSi is a quartet lying very close to the doublet state. The agreement we had with the three basis sets used allows one to assign the quartet state as the ground state of VSi conclusively.

Having obtained the desired basis set we apply the *ab initio* calculations to larger $\mathrm{V}_m\mathrm{Si}_n$ clusters. Our attempts to obtain stable V-encapsulated Si-cc by optimizing the clusters starting with $\mathrm{C}_{5\mathrm{v}}$ symmetry (found to be stable for the Ni-encapsulated Si-cc complex) were unsuccessful. Furthermore, the $\mathrm{VSi}_{10}$ cluster was found to be unstable on optimization starting with either $\mathrm{D}_{5\mathrm{h}}$ or $\mathrm{D}_{5\mathrm{d}}$ symmetry.

Recalling our experience with the different behaviour of Ni and V obtained in their bonding to graphite, and in particular the fact that V behaves as an $\eta^6$ ligand while Ni behaves as either an $\eta^2$ or $\eta^3$ ligand in their interaction with carbon (see for example [14]–[16, 33]), we were guided to investigate structures with $\mathrm{D}_6$ and $\mathrm{C}_6$ symmetries.

The $\mathrm{VSi}_{12}$ cluster with $\mathrm{D}_{6\mathrm{d}}$ symmetry was found to be unstable when optimized using the *ab initio* method. However, the $\mathrm{VSi}_{12}$ cluster in a slightly distorted $\mathrm{D}_{6\mathrm{h}}$ symmetry (see figure 3) was found to be stable with a ground state of doublet spin multiplicity. In this structure the Si–Si bond length in each hexagon is 2.370 Å, the Si–Si bonds connecting the two hexagons are 2.443 Å and the V–Si bond lengths range between 2.66 and 2.74 Å. Recalling from the VSi dimer data that the charge state of the V atom is approximately $+0.20|e|$, it is rather surprising to note that the charge state of the V atom in the $\mathrm{VSi}_{12}$ cluster is $-2.62|e|$, i.e., a large charge transfer to V from the surrounding Si atoms. This is an indication of the different hybridization

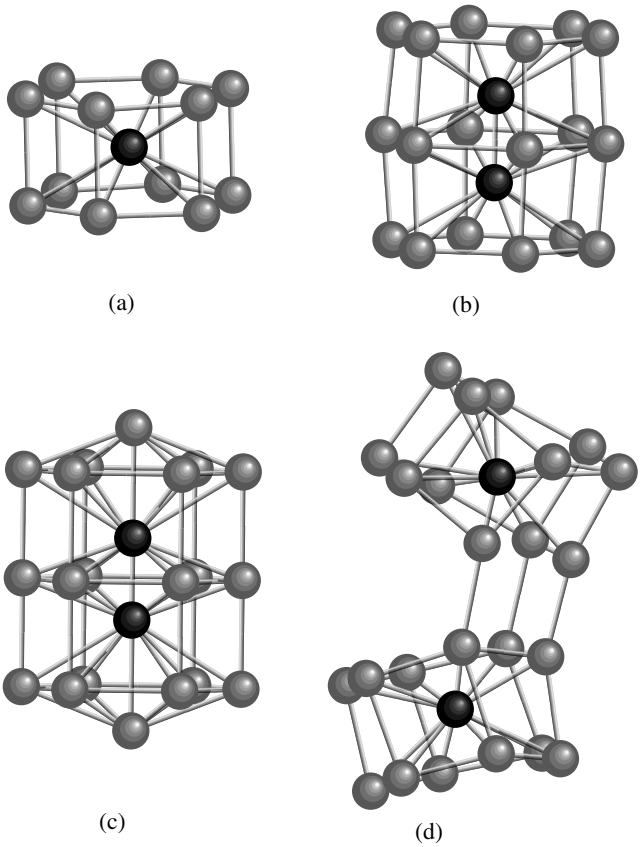


**Figure 3.** Relaxed Si-cc stabilized by encapsulating V atoms; $VSi_{12}$, $V_2Si_{18}$, $V_2Si_{20}$ and $V_2Si_{24}$. The V atoms are shown dark.

process taking place between V and surrounding Si atoms as the number of Si atoms (i.e., the coordination number of the V atom) is changed. The corresponding results for the $VSi_{12}$ cluster obtained from the TBMD simulations lead to slightly shorter V–Si bond lengths as compared to the *ab initio* ones. Furthermore, the V atom is found to exhibit a magnetic moment of $0.67\ \mu_B$ while the total spin of the cluster is $1\ \mu_B$.

The optimization of the $V_2Si_{18}$ cluster using the *ab initio* approach starting with a $D_{6h}$ symmetry resulted in a distorted $D_{6h}$ symmetry structure with both V atoms in a charge state of $-2.27|e|$.

These results lead us to conclude that the $VSi_{12}$ cluster is a highly stable unit forming strong V–Si bonds while weakening the Si–Si bonds between Si atoms belonging to adjacent Si hexagons. This is illustrated more graphically in the case of $V_2Si_{24}$ which, although optimized starting with $D_{6h}$ symmetry with the two V atoms far apart, relaxed into an oyster-like structure shown in figure 3. Another interesting feature was found from the TBMD study of the $V_2Si_{18}$ cluster and its end-capped version $V_2Si_{20}$; their relaxed structures are shown in figure 3. From these it is observed that the Si atoms forming the caps have a repelling effect on the V atoms, which come closer to each other in the capped structure. The V–V bond length in the capped structure is 1.86 Å, while in the uncapped case this is found to be 1.97 Å. The capping also results in smoothing out the expansion of the central hexagonal ring of Si atoms developed in the relaxed structure of the uncapped cluster.

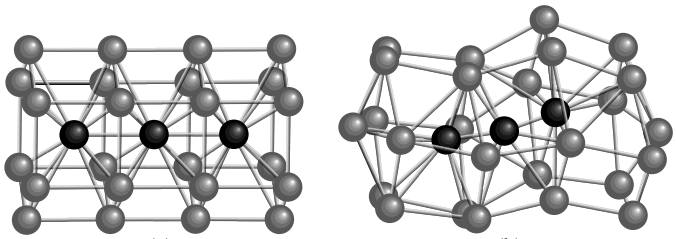


**Figure 4.** As in figure 3; relaxed Si-cc: $V_3Si_{24}$ and $V_3Si_{26}$. The V atoms are shown dark.

We next investigated the stability of larger $V_mSi_n$ clusters using only the TBMD method. This is because the *ab initio* approach for these clusters becomes computationally prohibitive as the number of the encapsulated TMAs increases. In these calculations, our primary aim is to check to see if one-dimensional V-encapsulated Si nanotubes are stable as was found in the case of Ni-encapsulated Si nanotubes. Towards this end we focused our investigations on testing the stability of V-encapsulated Si nanotubes built by adding successive $VSi_6$ units onto the stable $VSi_{12}$ cage cluster. We performed a stability analysis of V-encapsulated Si nanotubes of the general forms $V_nSi_{6n+6}$ (uncapped) and $V_nSi_{6n+8}$ (capped with Si atoms at both ends), each starting with $D_{6h}$ symmetry. For $n = 3$, it was found that the presence of capping atoms induces considerable frustration in the Si nanotube, which distorts into a puckered geometry. In the absence of end capping by Si atoms, however, the $V_3Si_{24}$ cluster is stable with almost perfect $D_{6h}$ symmetry (see figure 4). The distortions induced by the capped Si atoms become less pronounced as $n$ increases and both capped and uncapped tubes tend towards the same $D_{6h}$ symmetry. In these structures the V atoms retain their initial one-dimensional chainlike configuration as shown in figure 1(b).

The main features of the relaxed one-dimensional V-chain-encapsulated Si nanotubes were found to be as follows.

- The Si hexagons are at an average distance of 2.43 Å from each other.
- The V–V bond length exhibits a variation along the V chain; it alternates between a maximum (3.36 Å) and a minimum (1.92 Å) value. This difference decreases progressively as we approach the central V atoms of the chain. The lowest V–V distance appears between the end V atoms and their nearest V neighbour. This is followed by the largest V–V bond distance. This V–V bond variation may be attributed to the fact that the V–V (expected) bond length is much shorter than the shortest Si–Si bond lengths between Si hexagons.
- The V–Si bond length is in the range 2.60–2.97 Å.
- The tube diameter is mostly uniform (5.06 Å) along the tube length except at the two tube ends where it is slightly reduced.
- In contradistinction to the Ni encapsulation, in the V-encapsulated Si tubes the V atoms retain some magnetic moment ($\approx 0.65\ \mu_B$ per V atom).
- The V atoms tend to get electrons from the surrounding Si atoms and appear negatively charged with an excess electron charge of approximately $0.5|e|$ per V atom.

In figure 5 we present the $I$–$V$ curve for the $V_{13}Si_{84}$ nanotube in contact with two semi-infinite metal leads made of Ni(001). This curve was obtained using the same computational

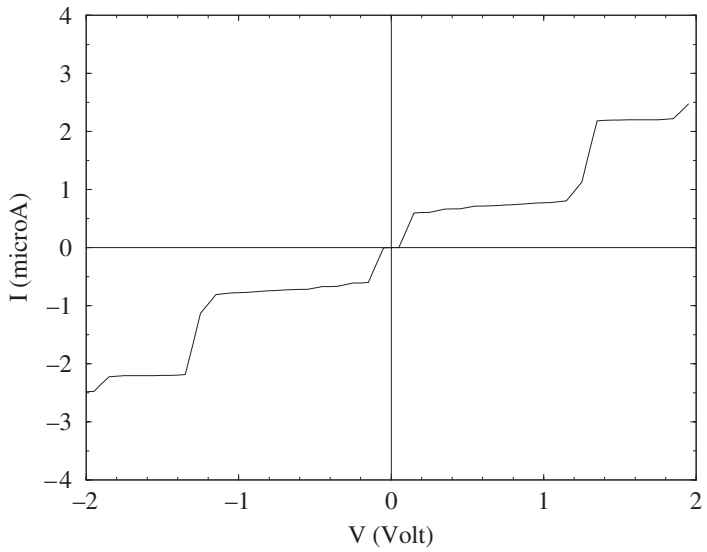


**Figure 5.** The $I$–$V$ characteristics under a symmetric bias of the Si nanotube shown in figure 1(b) as calculated according to to equations (6)–(9). The tube is in contact with semi-infinite metal leads made of Ni(001).

approach [26] as the one we used to obtain the $I$–$V$ curve of the $Ni_{15}Si_{80}$ tube shown in figure 2. As in the case of Ni encapsulation, the V-encapsulated Si nanotube appears to be almost metallic with a vanishingly small gap at $E_F$.

Finally, in figure 6 we show the calculated total and partial electron DOS for both systems, the $Si_{82}Ni_{15}$ and the $V_{13}Si_{84}$ metal-stabilized Si nanotubes. As is apparent from these graphs, the contribution of the d orbitals to the electron DOS at the Fermi energy is vanishingly small in the case for the encapsulated Ni chain and has non-negligible contribution in the case of V chain. Therefore, the contribution of the d-orbitals to the electron transport is found to depend on the kind of encapsulated material. Nevertheless, it appears that the conduction is mainly due to s and p orbitals as these are rehybridized in the present systems.

## 4. Discussion and conclusions

The results presented in the previous section confirm that TMAs interacting with Si exhibit contrasting bonding behaviour analogous to that found in the interaction of TMAs with low-dimensional C surfaces [14]–[17]. As revealed in the latter studies, the filling factor of the d band of the TMAs seems to play a significant role in this contrasting bonding behaviour. For example, both theory and experiment confirmed the tendency of early 3d series elements (Sc, Ti, V, Cr) to act as $\eta^6$ ligands, while the late 3d elements (Mn, Fe, Co, Ni) tend to act as $\eta^2$ and/or $\eta^3$ ligands when interacting with carbon surfaces. The present work shows evidence of analogous behaviour (although not identical) in the case of Si interacting with TMAs. The strong dependence of the TMA–Si interaction on the d-orbital occupancy and the coordination of the TMA is also evident in the data in table 2 where one can see that elements of the same group induce the same structural configuration on the encapsulating Si cage. This feature is more pronounced in small-size metal-encapsulated Si-cc where the bonding between metal and

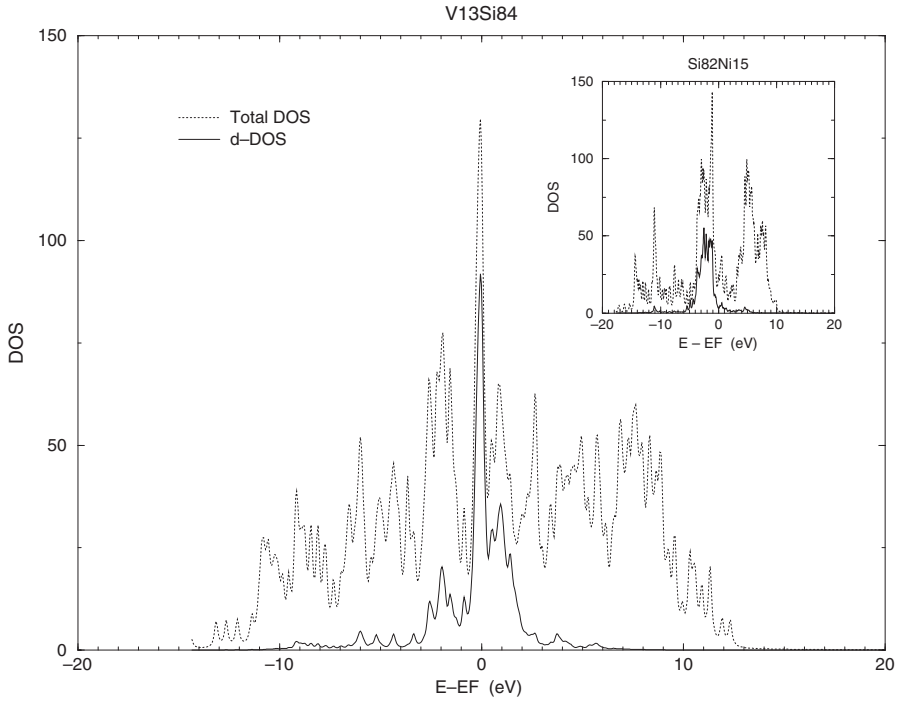


**Figure 6.** Total DOS (shown by the dashed curve) and partial (shown by the solid curve) d-electron DOS for the tube $V_{13}Si_{84}$ of figure 1(b). The corresponding curves for the tube $Si_{82}Ni_{15}$ are shown in the inset.

Si atoms is more restricted (and more sensitive to the coordination number of the TMA). Thus, in small-size metal-encapsulated Si-cc one can observe a change in the structure of the encapsulating Si cage as the filling factor of the d shell is changed (i.e. the d group is changed) but no structural changes as the size of the encapsulated metal atom changes (while remaining within the same d group). However, in larger Si-cc the size of the encapsulated atom may induce changes in the stability factor of the isomers of a given size Si-cc (as is apparent in the case of $MSi_{17}$; M = Cr, Mo, W).

One characteristic difference between the V-encapsulated Si-cc and the Ni-encapsulated ones appears in the effect of the Si encapsulation on the magnetic properties of the metal atoms. In particular, in the case of Ni, the encapsulation by Si leads to the passivation of the magnetic moment of Ni, while this does not happen in the case of V; the latter retains a considerable value of magnetic moment. However, in both cases, the magnetic moment of the Si-encapsulated metal atom is much less than the corresponding value of the free atom. As we have discussed in [16], it is worth emphasizing that the spin reduction of the encapsulated metal atom might have various contributions. It depends on the point group symmetry of the metal atom, the coordination number of the metal atom, the bond lengths between the metal atom and the neighbouring Si atoms, the charge transfer among them and consequently the relative shift of spin-up bands relative to spin-down ones and the population of the electron bands.

Not all of the stable Si-cc obtained can lead to the formation of Si-based nanotubes. However, Si-cc of certain special symmetries can evolve into long Si nanotubes. The symmetry of the Si-cc is dictated by the occupancy of the d orbital of the encapsulated TMAs. Thus, Ni-stabilized Si-cc of $C_{5v}$ symmetry were found to lead to stable Si-based nanotubes built up

from $NiSi_{10}$ units. Similarly, V-stabilized Si-cc of $D_{6h}$ symmetry can lead to the formation of Si-based nanotubes.

The approach of building up Si-based nanotubes using Si-cc as precursors is quite attractive and has been followed in some recently reported works. In particular, Marsen and Sattler [34] proposed the fullerene-like $Si_{24}$ as a building block for constructing Si nanotubes while Li *et al* have proposed as building blocks the tricapped and the uncapped trigonal prisms [8]. The Al-doped (encapsulated) fullerene-like $Si_{24}$ building unit was shown to lead to Si nanowires of better efficiency compared to Si nanowires based on the undoped fullerene-like $Si_{24}$ [35]. The present work as well as our preliminary report [9] have shown, for the first time, that encapsulated TMAs (of the 3d series) can in fact lead to Si-based nanotubes and demonstrated that a crucial factor which dominates this process is the filling factor of the 3d orbital of the TMA used. Furthermore, we have shown that studies referring to the interaction of TMAs with low-dimensional carbon surfaces can be used as a useful guide in the stability studies of metal-encapsulated Si-cc and Si-based nanotubes.

## Acknowledgments

The present work is supported through grants by the NSF (NER-0165121), DOE (00-63857), NASA (02-465679), the EU-GROWTH research project AMMARE (G5RD-CT-2001-00478) and the University of Kentucky Center for Computational Sciences.

## References

[1] Shinobara H 2000 *Rep. Prog. Phys.* **63** 843
[2] Menon M and Subbaswamy K R 1994 *Chem. Phys. Lett.* **219** 219
[3] Hiura H, Miyazaki T and Kanayama T 2001 *Phys. Rev. Lett.* **86** 1733
[4] Ovcharenko I V, Lester W A Jr, Xiao C and Hagelberg F 2001 *J. Chem. Phys.* **114** 9028
[5] Andriotis A N, Menon M and Froudakis G 1999 *J. Cluster Sci.* **10** 549
[6] Kumar V and Kawazoe Y 2001 *Phys. Rev. Lett.* **87** 045503
[7] Kumar V and Kawazoe Y 2002 *Phys. Rev.* B **65** 073404
[8] Li B-X, Cao P-L, Zhang R Q and Lee S T 2002 *Phys. Rev.* B **65** 125305
[9] Menon M, Andriotis A N and Froudakis G 2002 *Nanoletters* **2** 301
[10] Andriotis A N and Menon M 1998 *Phys. Rev.* B **57** 10069
[11] Slater J C and Koster G F 1954 *Phys. Rev.* **94** 1498
[12] Harrison W 1980 *Electronic Structure and Properties of Solids* (San Francisco, CA: Freeman)
[13] Frisch M J *et al* 1998 *Gaussian 98* revision A.6 (Pittsburgh, PA: Gaussian)
[14] Andriotis A N, Menon M, Froudakis G E and Lowther J E 1999 *Chem. Phys. Lett.* **301** 503
[15] Andriotis A N and Menon M 1999 *Phys. Rev.* B **60** 4521
[16] Andriotis A N, Menon M and Froudakis G E 2000 *Phys. Rev.* B **62** 9867
[17] Andriotis A N, Menon M and Froudakis G E 2000 *Chem. Phys. Lett.* **320** 425
[18] Froudakis G E, Muhlhauser M, Andriotis A N and Menon M 2001 *Phys. Rev.* B **64** 241401(R)
[19] Nagao S, Kurikawa T, Miyajima K, Nakajima A and Kaya K 1998 *J. Chem. Phys.* A **102** 4495
[20] Kurikawa T, Nagao S, Miyajima K, Nakajima A and Kaya K 1998 *J. Chem. Phys.* A **102** 1743
[21] Nakajima A, Nagao S, Takeda H, Kurikawa T and Kaya K 1997 *J. Chem. Phys.* **107** 6491
[22] Parks E K, Kerns K P, Riley S J and Winter B J 1999 *Phys. Rev.* B **59** 13431
[23] Mathur P, Mavunkal I J and Umbarkar S B 1998 *J. Cluster Sci.* **9** 393
[24] Andriotis A N, Menon M, Froudakis G, Fthenakis Z and Lowther J E 1998 *Chem. Phys. Lett.* **292** 487

[25] Jackson K and Nellermoe B 1996 *Chem. Phys. Lett.* **254** 249
[26] Andriotis A N and Menon M 2001 *J. Chem. Phys.* **115** 2737
[27] Landauer R 1987 *Z. Phys.* B **68** 217
[28] Datta S 1995 *Electronic Transport in Mesoscopic Systems* (Cambridge: Cambridge University Press)
[29] Inglesfield J E 1981 *J. Phys. C: Solid State Phys.* **14** 3795
[30] Fisher A J 1990 *J. Phys.: Condens. Matter* **2** 6079
[31] Andriotis A N 1992 *Europhys. Lett.* **17** 349
[32] Andriotis A N 1990 *J. Phys.: Condens. Matter* **2** 6079
[33] Duffy D M and Blackman J A 1998 *Phys. Rev.* B **58** 7443
[34] Marsen B and Sattler K 1999 *Phys. Rev.* B **60** 11593
[35] Landman U, Barnett R N, Scherbakov A G and Avouris Ph 2000 *Phys. Rev. Lett.* **85** 1958